



## Research article

# Copper oxide nanoflowers/poly-L-glutamic acid modified advanced electrochemical sensor for selective detection of L-tryptophan in real samples

M.A. Khaleque<sup>a,b</sup>, M.S. Bacchu<sup>a,b</sup>, M.R. Ali<sup>a,b</sup>, M.S. Hossain<sup>a,b</sup>, M.R.A. Mamun<sup>a,b</sup>, M.I. Hossain<sup>a,b</sup>, M.Z.H. Khan<sup>a,b,\*</sup>

<sup>a</sup> Dept. of Chemical Engineering, Jashore University of Science and Technology, Jashore, 7408, Bangladesh

<sup>b</sup> Laboratory of Nano-bio and Advanced Materials Engineering (NAME), Jashore University of Science and Technology, Jashore, 7408, Bangladesh

## ARTICLE INFO

## Keywords:

Copper oxide nanoflower  
Poly-L-glutamic acid  
L-tryptophan  
Cyclic voltammetry  
Electrochemical sensor

## ABSTRACT

The main objective of this research work is to develop a low-cost sensor to detect L-tryptophan (L-tryp) in real sample medium based on a modified glassy carbon electrode. For this, copper oxide nanoflowers (CuONFs) and poly-L-glutamic acid (PGA) were used to modify GCE. The prepared NFs and PGA coated electrode was characterized using field emission scanning electron microscope (FE-SEM) with energy dispersive X-ray (EDX) and attenuated total reflectance Fourier transform infrared (ATR-FTIR) spectroscopy. Furthermore, the electrochemical activity was performed by cyclic voltammetry (CV), differential pulse voltammetry (DPV) and electrochemical impedance spectroscopy (EIS). The modified electrode showed excellent electro-catalytic activity towards L-tryp detection in PBS solution at neutral pH 7.0. Based on the physiological pH condition, the proposed electrochemical sensor can detect L-tryp concentration with a linear range of  $1.0 \times 10^{-4}$ – $8.0 \times 10^{-8}$  molL<sup>-1</sup> with having a detection limit of  $5.0 \times 10^{-8}$  molL<sup>-1</sup> and sensitivity of 0.6 μA/μMcm<sup>2</sup>. The selectivity of L-tryp was tested with a mixture of salt and uric acid solution at the above conditions. Finally, this strategy demonstrated excellent recovery value in real sample analysis like milk and urine.

## 1. Introduction

L-tryptophan (L-tryp) is an alanine derivative substance that contains, α-amino, and α-carboxylic acid functional group and side chain indole ring on β carbon which is essential for the synthesis of hormones, serotonin, melatonin, niacin, auxin and vitamin B<sub>3</sub> for human beings [1]. In addition, L-tryp has a group of functions to retain optimum human body conditions as like for mood enhancement, antidepressant, and nutraceutical behaviors [2]. Generally, it is used to treat sleep problems (insomnia), anxiety, depression, premenstrual tension, and attention deficit disorder by whom cannot produce it by metabolic pathway [3]. Based on the literature, relatively higher L-tryp (19 mg/kg/day) is needed for fast growing infant whereas children aged (10–12 years) and adults require at least 4 mg/kg/day and 3 mg/kg/day respectively [4]. The higher consumption of L-tryp causes hyperthyroidism while lower leads to various diseases such as hypochondria, confusion, dementia, hyperthyroidism, parkinson's and albinism [3,5]. In this regard, L-tryp is often added as a fortifier to diet, food and pharmaceutical preparations. However, the detection of L-tryp in blood fluid is a

\* Corresponding author. Dept. of Chemical Engineering, Jashore University of Science and Technology, Jashore, 7408, Bangladesh.  
E-mail address: [zaved.khan@yahoo.com](mailto:zaved.khan@yahoo.com) (M.Z.H. Khan).

<https://doi.org/10.1016/j.heliyon.2023.e16627>

Received 19 July 2022; Received in revised form 10 May 2023; Accepted 22 May 2023

Available online 24 May 2023

2405-8440/© 2023 Published by Elsevier Ltd.

This is an open access article under the CC BY-NC-ND license

(<http://creativecommons.org/licenses/by-nc-nd/4.0/>).

robust and reliable method and has received potential interest from researchers in last few decades.

Various analytical methods like spectrophotometry [6,7], high performance liquid chromatography [8,9], fluorescence [10], chemiluminescence [11], and capillary electrophoresis [12], have been employed for the detection of L-tryptophan in food, plasma, urine, and other biological media. Some drawbacks have been formulated in mentioned methods such as time-consuming, instrument handling, and high cost of reagents. To address these difficulties, electrochemical analytical tools have received much more acceptance to their greater simplicity, selectivity in design and fabrication, quick response, availability and cheapness for the detection of L-tryptophan [13]. Hence, we have reported the electrochemical method for the detection of L-tryptophan with a simple electrode modification process comparing with other research methods. Though L-tryptophan exhibited a slow electrochemical response over higher oxidation potential, a considerable number of studies have been done for enhancing the detection of L-tryptophan followed by chemically modified electrode [14]. For instance, He et al. (2019), reported on a modification of GCE with cuprous oxide and electrochemically reduced graphene oxide composite for L-tryptophan detection by a square-wave voltammetry (SWV) method [15]. The modified electrode, exhibited the oxidation voltogram of 10  $\mu\text{M}$  L-tryptophan in 0.05 M  $\text{H}_2\text{SO}_4$  and the peak in the mixture of 1.0 mM AA, 10  $\mu\text{M}$  dopamine, and 10  $\mu\text{M}$  uric acid respectively. Zhu et al. (2014), demonstrated an electrochemical sensor of GCE modified with single-walled carbon nano horns (SWCNHs) for direct and quantitative L-tryptophan detection in spiked serum samples [16]. Another researchers, Khoshnevisan et al. (2020), fabricated GCE by using reduced graphene oxide (rGO) layered by 18-crown-6 with gold nanoparticles for L-tryptophan detection in the diabetic patient and normal human serum [17]. The SWV method was utilized in the presence of interfering glucose, dopamine, ascorbic acid, and urea. Porifreva et al. (2018), reported the utilization of silver nanoparticles in polyactide-thiocalix [4] arene copolymer on GCE for electrochemically (0.1–100  $\mu\text{M}$ ) L-tryptophan detection [18]. Furthermore, Boonchiangma et al. (2014), were proposed a screen printed electrode which was fabricated by electropolymerization of *p*-phenylene-diamine and thereafter covalently bonded with cysteamine capped cadmium sulfide quantum dots by using glutaraldehyde cross-linker [19]. The forming organic-inorganic hybrid composite film has an electrochemical response to detecting L-tryptophan over other amino acids. However, most of the L-tryptophan detection studies were reported complex fabrication procedures that indicates time consuming and costly.

Recently, metal oxide nanoparticles have received considerable attention to prepare chemically modified electrodes due to their high catalytic activity, high conductivity, better stability and cheap cost. In particular, most researchers have focused on copper oxide nanoparticles (CuONPs) because its higher conductivity, bioavailability, Universalizability, etc. [20,21]. Different sizes and shapes of CuONFs (nanoballs, nanoparticles, nanospheres, nanosheets, nanotubes, nanorods etc.) have been synthesized to obtain a wide range of electro-catalytic performance [22–25]. At this point, cyclic voltammetry is the most popular and common electrochemical method for a stable structure and dimension on a support [26–32] by applying suitable current. The active surface area was increased with the deposition of nanoparticles, and consequently enhanced the electrocatalytic activity [31].

The use of non-essential amino acid polymer in the electrochemical system has received greater potential in the last few decades due to excellent characteristics including excellent perm-selectivity, more active sites, strong adherence to the electrode surface, and good stability [33,34]. The biosynthesized polymer was much more trendy for sensor fabrication to detect biomolecules compared to the artificial polymer as they are bio-compatible as well as bio-degradable properties [35–37]. The poly-glutamic acid (PGA) is such type of biopolymer which have versatile applications [38–43]. Besides, poly-glutamic acid monosodium (PGA) behave as a conducting bridge by rapid electron transformation [44–46]. In the polymer chain,  $\gamma$ -peptide bonds were formed between the  $\alpha$ -amino and  $\alpha$ -carboxylic acid functional groups where monosodium-carboxyl groups remain unchanged [46–48]. Therefore, the PGA shows superior conductivity in the field of electrochemical modification [46,49].

In this research work, CuONFs and PGA modified electrochemical glassy carbon electrode (GCE) sensor were proposed for sensitive and selective detection of L-tryptophan. Similarly, the designed sensor was used to detect a different concentration of L-tryptophan in an experimental condition because of negatively charged PGA surface and positively charged L-tryptophan in 0.01 M PBS (pH 7.0). This research group was trying to find out low cost and very easy modifications for the detection of vital amino acids (L-tryptophan). Many articles were studied to perform this types of less complex work specially focusing on to find out an easy process. Finally, the selectivity performance was analyzed in a mixture of salt and uric acid solution.

## 2. Materials and methods

### 2.1. Chemicals and materials

The maximum integrity chemicals were purchased for this research purpose. L-tryptophan (purity 99.5%) was purchased from Sigma-Aldrich (China), L-glutamic acid (monosodium salt) (purity 99%) from Sisco Research Laboratories Pvt. Ltd (India), Cupric sulfate pent hydrate (purity 99%) and polyvinyl pyrrolidone (PVP) from Loba Chemie Pvt Ltd (India), Hydrogen peroxide from Pt. Smart Lab (Indonesia). Type I with resistivity <18 M $\Omega$  double distilled ultrapure water was made from Evoqua (Germany) and was used during total experiments. A supporting electrolyte of phosphate-buffered saline (PBS) was purchased from Sigma Aldrich (China). Moreover, analytical grade reagents and chemicals were used in this experiment with high purity. Each electrolyte solution was deoxygenated for 5 min before voltammetry measurement.

### 2.2. Synthesis of CuONFs

An effective hydrothermal method was followed to synthesize CuONFs and a process was proposed according to the previous report with some modifications. At first, copper sulfate pent hydrate (1 g) was dispersed into 200 mL of doubled distilled and ultrapure water in a beaker. Afterward, 500 mg of PVP was added slowly into the solution with vigorous stirring control temperature. In the following

step, 40 mL of 0.2 M NaOH was added dropwise, and a blue suspension was formed. At last, 150  $\mu\text{L}$  hydrazine hydrate solution (80 wt %) was added to the mixture and stirred for 20 min at room temperature (25  $^{\circ}\text{C}$ ) until to obtain brick red mixture. The obtained suspended solution was centrifuged several times and washed with ultrapure water and absolute ethanol to improve the phase separation. Finally, the resulting sample was dried overnight at 60  $^{\circ}\text{C}$  to remove moisture and other organic materials. The obtaining sample was marked as pure CuONFs after grinding and ready to use for analytical purposes.

### 2.3. Fabrication of GCE/CuONFs/PGA

To clean the GCE surface, 0.1, 0.3 and, 0.05  $\mu\text{m}$  of  $\text{Al}_2\text{O}_3$  powder was used on the polishing pad and the polishing time was at least 1 min. After that, the electrodes surface were rinsed ultrasonically individually for 3 min in DI water and ethanol to remove adhering pollutants, and alumina particles. The acid treatment of GCE was performed in 0.8 M sulfuric acid at (–1 to 1) V with a scan rate of 100  $\text{mVs}^{-1}$  for 23 cycles by cyclic voltammetry (CV) and dried in the open air. Then, the electrode was dipped in 0.01 M of PBS (pH 7.0), containing 0.15  $\text{mgmL}^{-1}$  of CuONFs solution for electrodeposition. To prepare the GCE/CuONFs electrode a potential range from –1.4 to 0.7 (at 100  $\text{mVs}^{-1}$  for 15 cycles) was applied by CV. After electrodeposition, the modified electrode was rinsed with ultrapure water and quickly used for further modification. In this case, a 50 mM of Glutamic acid in PBS (pH 7.0) solution was electro polymerized on the electrode surface between –1.4 and 2.0 V at the 100  $\text{mVs}^{-1}$  for 15 cycles through cycling voltammetry. All the working procedure is represented in Scheme 1. Finally, the modified electrode was rinsed with ultrapure water and carefully stored and called the GCE/CuONFs/PGA electrode.

### 2.4. L-tryptophan (L-tryp) measurement procedure

All electrochemical measurement of L-tryp was performed using electrochemical workstation (Corr Test CS300, China) by differential pulse voltammetry (DPV) technique. For this measurement, 10 mL of different concentration of L-tryp in 0.01 M PBS (pH 7.0) was prepared and measured as prepared GCE/CuONFs/PGA electrode. The L-tryp in real samples DPV response also measured to dilute the real samples into ten times in 0.01 M PBS (pH 7.0). The total working procedure is represented in Scheme 1.

### 2.5. Apparatus and instruments

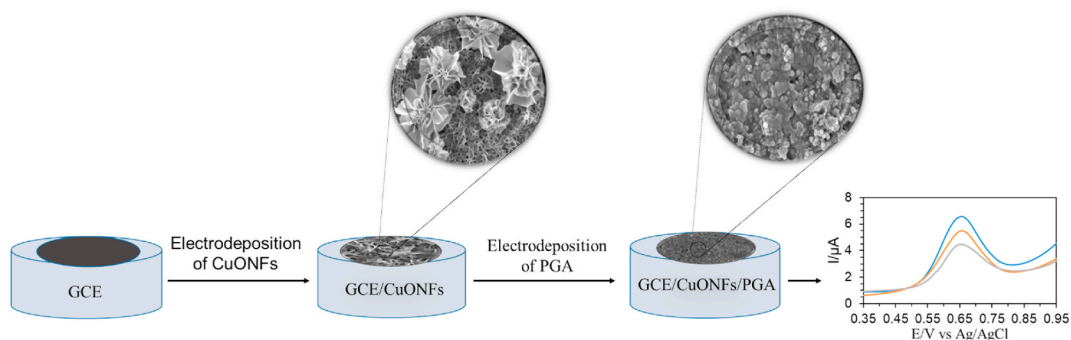
All glassware in this experiment was treated with 10% nitric acid for 24 h and dried at 60  $^{\circ}\text{C}$ . The voltammetry procedure was done by an electrochemical workstation (Corr Test CS300, China). The surface morphology with individual elemental composition and functional groups were characterized by scanning electron microscopy (ZEISS Gemini SEM 500 (UK)) and attenuated total reflectance fourier transform infrared (ATR-FTIR) (NICOLET iS20, USA) spectroscopy analyses respectively. Electrochemical impedance spectroscopy (EIS) was measured by Metrohm DropSens ( $\mu\text{Stat-I 400 s S/N: IS4091044A}$ , Switzerland). The  $\text{N}_2$  atmosphere was maintained to conduct all types of voltammetry procedures.

## 3. Results and discussion

### 3.1. Surface morphology and functional group study of CuONFs

The surface morphology with elemental composition and functional groups of the prepared electrode surface is shown in Fig. 1. As shown in Fig. 1A, a flower-like surface morphology was demonstrated. A large view of CuONFs is shown in Fig. 1B and the average particle size was measured and found to be 2–8  $\mu\text{m}$ . A relatively rough surface and irregular shape with uniform distribution were exhibited the addition of PGA into CuONFs solution (Fig. 1C).

As shown in Fig. 1E, the peak observed at 511.37, 630.13  $\text{cm}^{-1}$  were denotes as stretching vibrations of Cu–O band which confirmed the formation of CuONFs [50]. The peak at 870.75  $\text{cm}^{-1}$  was assigned to the stretching vibrations of C–H bond [50] and



**Scheme 1.** Systematic representation of electrode modification for L-tryptophan detection.

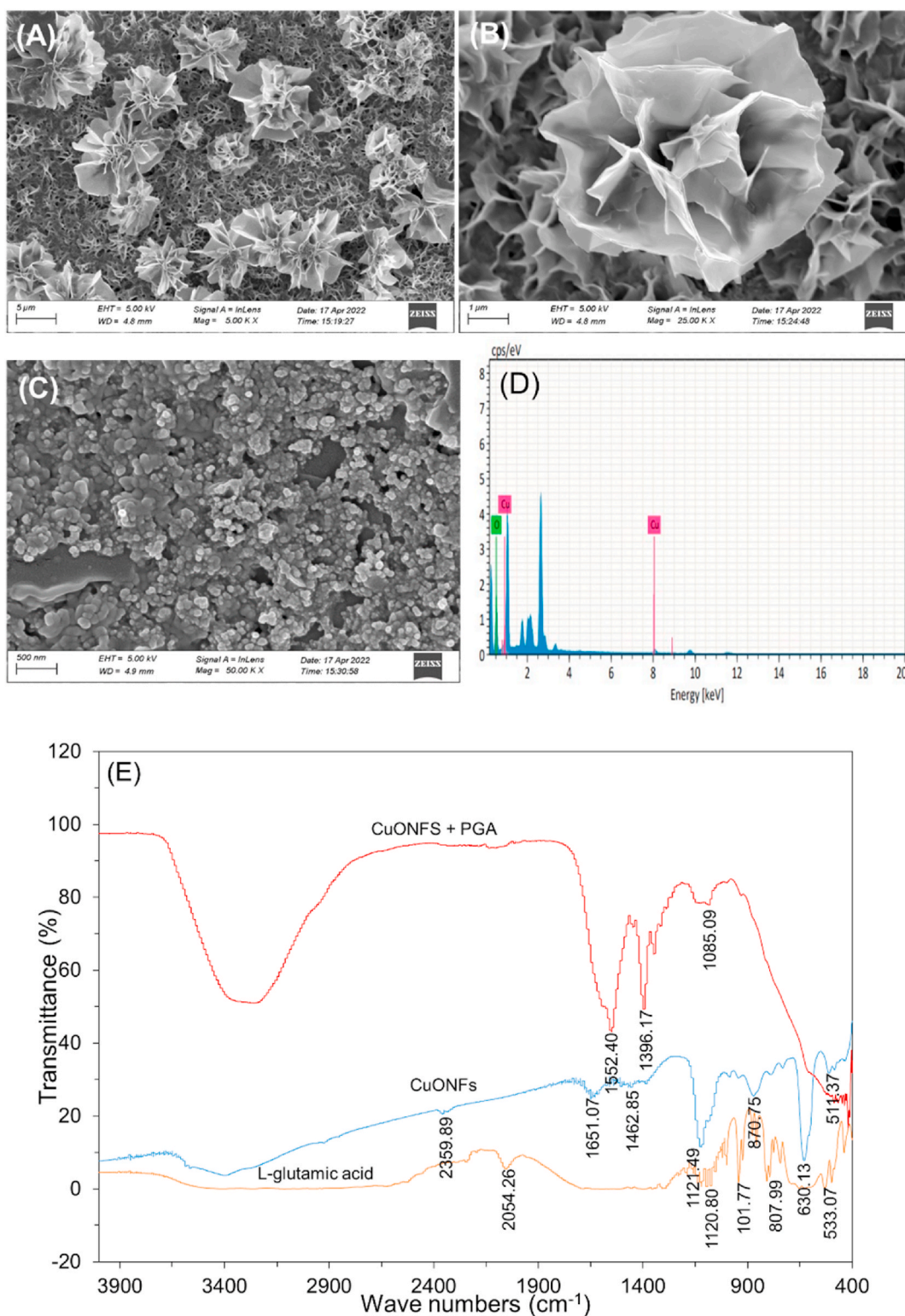


**Fig. 1.** SEM images of (A) bare GCE/CuONFs; (B) bare GCE/CuONFs/PGA. (C) ATR-FTIR spectrum of L-glutamic acid, CuONFs, and CuONFs + PGA. (D) EDX figure of CuONFs where the bright spot show the distribution of Cu and O elements on the electrode.

1121.49  $\text{cm}^{-1}$  vibration was formed due to the due to degenerative mode of  $\text{SO}_4^{2-}$  ions [51]. Another peak at 1462.85, 1651.07  $\text{cm}^{-1}$  was attributed to the bending vibration of O–H band of CuONFs which was adsorbed by water molecules [51]. In addition, L-glutamic acid (monosodium) has shown multiple vibrations with a broad spectrum from 438.66 to 3109.22  $\text{cm}^{-1}$ . In the study of CuONFs and L-glutamic acid nanocomposite, CuONFs made a complex with PGA these are proved by 436.34, 418.87 and 401.26  $\text{cm}^{-1}$ . The rest of the 1085.09, 1346.48, and 1396.17  $\text{cm}^{-1}$  peaks were assigned as the vibration of C–N, C–H, and C–O bonds respectively. Another, stretching vibration of N–H was founded at 1552.40  $\text{cm}^{-1}$  wave number [52]. Based on EDX analysis, the CuONFs proved that the electrode surface was decorated with flowers. The EDX surface distributions confirmed the presence of Cu and O as shown in Figure (1 D).

### 3.2. Electrodeposition of CuONFs-PGA

The synthesized CuONFs was electrodeposited on the bare GCE at a potential range (–1.4 to 0.7) V with a scan rate of 100  $\text{mVs}^{-1}$  for 15 cycles by using CV technique [53]. The CuONFs deposition on GCE is shown in Fig. 2. As shown in Fig. 2A, the oxidation of CuONFs can be notified from the cycling voltammogram with a large anodic peak current near zero volts. Additionally, the electrode position of PGA was conducted by a CV with a voltage ranging from –1.4 to 2.0 V (at 100  $\text{mVs}^{-1}$  for 15 cycles) at 0.01 M of PBS (pH 7.0) solution [45,54,55]. Fig. 2B shows the deposition cycle of the L-glutamic acid monosodium on GCE/CuONFs electrode. The polymerization of L-glutamic acid on the GCE surface occurred at about +1.75 V with a high peak which was demonstrated by researcher [55]. The L-glutamic acid monomer was spontaneously polymerize on the surface of the deposited CuONFs electrode through a covalent linkage [56]. The successive increase of oxidation peak height was evident that the deposition of PGA in favor of increase electrode conductivity. For the optimization of effective electrodeposition of L-glutamic acid was studied at the scan rate of 100  $\text{mVs}^{-1}$  for 15 cycles by CV technique with preparing different concentrations.

### 3.3. Effect of L-glutamic acid concentration and pH

From Fig. 2 CuONFs and PGA were electrodeposited on acid activated GCE. In which PGA electro-polymerization is optimized using different concentration of L-glutamic acid with a potential range (–1.4 to 0.7) V with a scan rate of 100  $\text{mVs}^{-1}$  for 15 cycles. In Fig. 3 it is found that 50 mM L-glutamic acid exhibited maximum oxidation compared with 30, 40, 60, 70, and 80 mM concentrations. This result ascribed the thicker layer of PGA is suitable for oxidation L-trypt than the excess and lower ones. Similarly, in the study of pH effect in PBS medium we exhibited at acidic and basic conditions the oxidation of L-trypt is lower but at neutral pH 7.0 it is highest. Hence, physiological pH 7.0 is chosen for the detection of L-trypt in real samples medium.

### 3.4. Electrochemical behavior of GCE/CuONFs/PGA in $\text{Fe}(\text{CN})_6^{3-/4-}$

As shown in Fig. 4 (A-C), the electrochemical characterization of bare GCE, GCE/CuONFs, and GCE/CuONFs/PGA electrode followed by CV in 0.1  $\text{molL}^{-1}$  of KCl and 0.005  $\text{molL}^{-1}$  of  $\text{Fe}(\text{CN})_6^{3-/4-}$ . By casting an eye on Fig. 4A, the lowest peak current with a well-defined redox peak was obtained for bare GCE with having peak to peak potential separation value ( $\Delta E_p$ ) of 137 mV. At a time, it was 104 mV for GCE/CuONPs electrode, and 79.6 mV for CuONFs/PGA modified GCE/CuONFs/PGA increase diffusion redox rate of  $\text{Fe}(\text{CN})_6^{3-/4-}$ . Additionally, another researcher reported the homogeneous film of CuONFs that have the property to increase the electron mobility [57] comparing with the bare GCE using the Nyquist plot (Fig. 4B). In this work, the modified GCE/CuONFs/PGA electrode exhibited the lowest impedance (15  $\Omega^{-1}$ ) in 0.1  $\text{molL}^{-1}$  of KCl including 0.005  $\text{molL}^{-1}$  of  $\text{Fe}(\text{CN})_6^{3-/4-}$  compared with GCE/CuONFs (630  $\Omega^{-1}$ ) and bare GCE (700  $\Omega^{-1}$ ) due to an increase of active surface area and conductivity of the modified electrode. As a reason, the GCE/CuONFs/PGA electrode maintained the lowest electron transfer resistance ( $R_{ct}$ ), electrolyte resistance ( $R_s$ ), and capacitance of double layer ( $C_{dl}$ ) [58–60]. From Fig. 4B the semicircle exhibited the highest resistivity in contrast, the linear line without semicircle showed the lowest resistivity. Moreover, the electro polymerized film of L-glutamic acid on CuONFs maintains a synergetic effect that renders the electron transfer kinetics [61].

Additionally, the cyclic voltammetry from 0.2 to 0.6 V with decreasing scan rate from outer to inner (200, 150, 100, 90, 80, 70, 60,

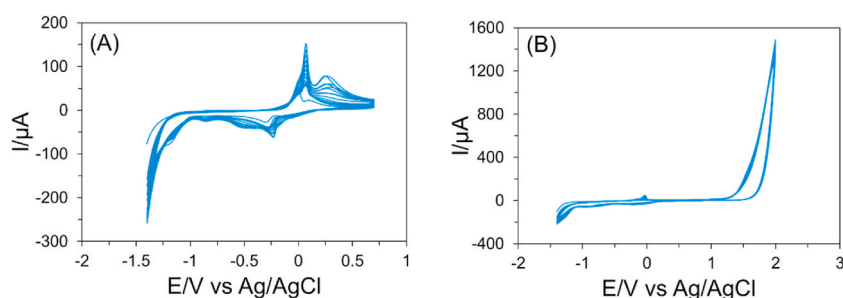


**Fig. 2.** Cyclic voltammograms at a scan rate of 100  $\text{mVs}^{-1}$  for 15 cycles in PBS pH 7.0 for the (A) electrochemical deposition/reduction of CuONFs on bare electrode; (B) electrochemical polymerization of 50 mM L-glutamic acid on the GCE/CuONFs electrode.

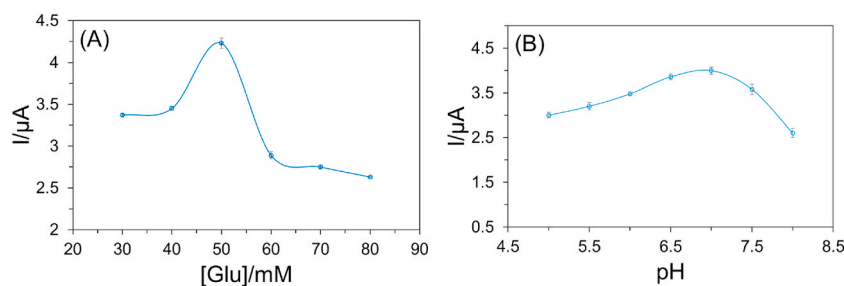


**Fig. 3.** Effect on the oxidation of  $1.0 \times 10^{-4} \text{ mol L}^{-1}$  L-tryptophan A) concentration of L-glutamic acid; B) different pH values.

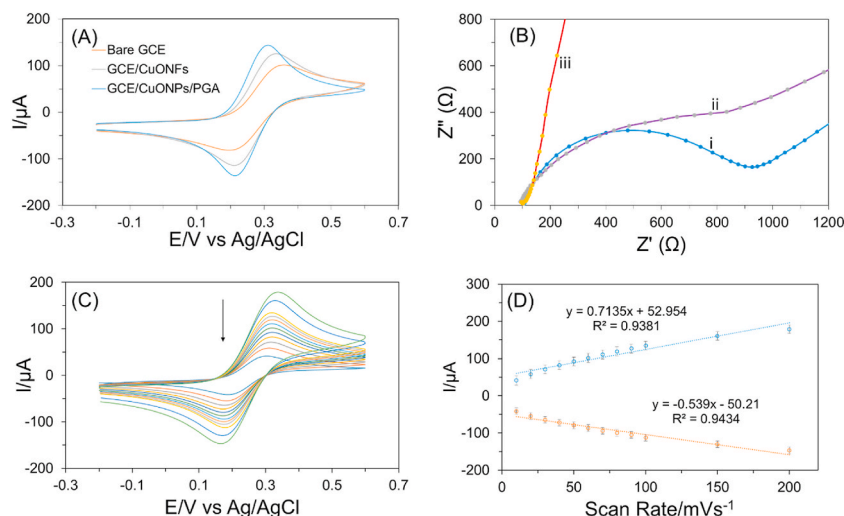


**Fig. 4.** Cyclic voltammograms of different electrodes measured in  $0.1 \text{ mol L}^{-1}$  of KCl including  $0.005 \text{ mol L}^{-1}$  of  $\text{Fe}(\text{CN})_6^{3-/4-}$  (A): bare GCE, GCE/CuONFs, and GCE/CuONFs/PGA; (B): EIS images of (i) bare GCE, (ii) bare GCE/CuONFs, and (iii) GCE/CuONFs/PGA; (C): CV at different scan rates (from outer to inner): 200, 150, 100, 90, 80, 70, 60, 50, 40, 30, 20, and  $10 \text{ mVs}^{-1}$  and (D) the corresponding calibration plots between different scan rates versus anodic ( $I_{pa}$ ) and cathodic peak current ( $I_{pc}$ ).

50, 40, 30, 20, and  $10 \text{ mVs}^{-1}$ ) was also represented in Fig. 4C. It was noticeable that the peak current gradually decreases with minimizing the scan rate. It confirmed the ion transfer phenomenon which was controlled by absorption. According to the literature, polymer coated metal particles, enhanced the sensitivity, and stability of the sensor [62]. The corresponding calibration line of 4. C is shown in Fig. 4D which maintained the rising oxidation increasing and gradual decreasing of reduction current value. These two lines maintained the satisfactory  $R^2$  value. Moreover, Randles sevcik equation was used to calculate the active surface area (A) of different electrodes. The calculated A value for the bare GCE, GCE/CuONFs, and GCE/CuONFs/PGA electrodes were  $0.112 \text{ cm}^2$ ,  $0.154 \text{ cm}^2$  and  $0.452 \text{ cm}^2$  respectively.

### 3.5. Electrochemical detection of L-tryptophan

As shown in Fig. 5A, differential pulse voltammetry (DPV) analysis of  $1.0 \times 10^{-4} \text{ mol L}^{-1}$  of L-tryptophan was investigated in  $0.01 \text{ M}$  PBS (pH 7.0) for bare GCE, GCE/PGA, and GCE/CuONFs/PGA. It can be seen that the successive peak height was gradually increased with the modification of PGA and CuONFs in GCE. In this study, the modified GCE/CuONFs/PGA behaved as a negatively charged surface and L-tryptophan as positive surface which is the main detection mechanism of L-tryptophan. The electrochemical reaction of L-tryptophan oxidation is shown in Scheme 2.

Additionally, successful responses were monitored in the case of a different range of analytic concentration. It was observed that the oxidation current increases proportionally with increasing concentration of L-tryptophan a range of  $8.0 \times 10^{-8} - 1.0 \times 10^{-4} \text{ mol L}^{-1}$  by plotting the anodic peak in Fig. 5B. Therefore, an excellent correlation was maintained between L-tryptophan concentrations and oxidation current. Furthermore, the linear concentration versus obtained data using regression equation  $y = 0.0417x + 0.2588$  ( $R^2 = 0.9929$ ) with a detection limit of  $5.0 \times 10^{-8} \text{ mol L}^{-1}$  was observed. This lower concentration reported that the GCE/CuONFs/PGA electrochemical sensor denoted linearity and comparatively the lowest detection limit.

We compared our research outcome to other published modified electrodes for further studies are summarized in Table 1. The modified GCE/CuONFs/PGA sensor was shown notable benefits including acceptable linear range, low detection limit, and high

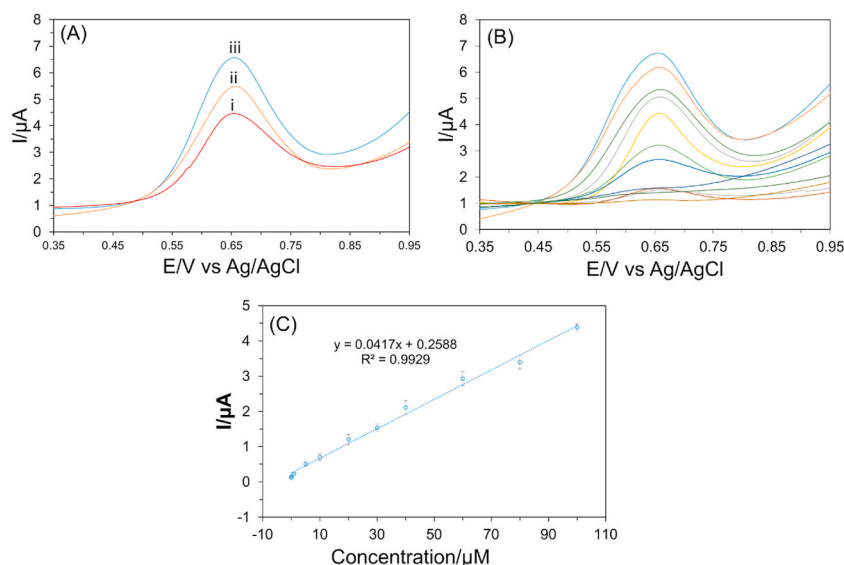
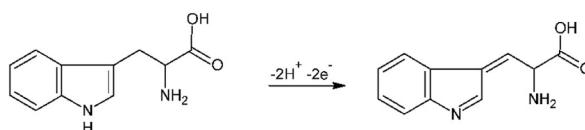


**Fig. 5.** DPV response by using the GCE/CuONFs/PGA in PBS solution (pH 7.0) for (A) 100  $\mu\text{M}$  of L-trypt (i) bare GCE; (ii) GCE/CuONFs; and (iii) bare GCE/CuONFs/PGA (B) L-trypt concentration range from  $1.0 \times 10^{-4}$ – $8.0 \times 10^{-8}$   $\text{molL}^{-1}$  with inset the calibration curve; (C) the corresponding calibration curve of Fig. 5(B).



**Scheme 2.** Electrochemical oxidation of L-trypt at GCE/CuONFs/PGA modified electrode.

**Table 1**

Comparison of GCE/CuONFs/PGA sensor for L-tryptophan detection with other published modified electrodes.

Methods	Linear range ( $\mu\text{M}$ )	Detection limit ( $\mu\text{M}$ )	References
Butrylcholine/GCE	2–60	0.6	[63]
Hemin/GCE	0.1–100	0.025	[64]
CNF/CPE	0.1–118.5	0.1	[65]
PG/CNTPE	0.05–100	0.1	[66]
NiO/CNT/PEDOT/GCE	1–41	0.210	[67]
NiCo <sub>2</sub> O <sub>4</sub> /Nano-ZSM-5	0.9–1000	0.7	[68]
PTh/GCE	6–180	0.6	[69]
TiO <sub>2</sub> -GR/4-ABSA/GCE	1–30	0.3	[70]
MWCNT-CPE/GCE	0.6–9.0; 10–100	0.03	[71]
ERGO/GCE	0.2–40	0.1	[72]
SWCNH/GCE	0.5–50	0.05	[16]
NOMAC/Nafion/GCE	0.5–70; 70–200	0.035	[73]
NPC/GCE	1–103	0.03	[74]
AgNPs/P(L-Arg)-GO/GCE	1–150	0.407	[75]
MB/Ag-ZnO/GR/GCE	2–140	1.0	[76]
PGA/CuONFs/GCE	0.08–100	0.05	<b>This work</b>

sensitivity.

### 3.6. Selectivity, reproducibility, and stability study

To evaluate the practical application, selectivity, stability, and reproducibility are the most crucial matter. Fig. 6 represent the experiment output of the following analysis. The selectivity of PGA/CuONFs/GCE sensor was investigated using an interfering salt solution (cation and anion) in  $1.0 \times 10^{-4}$   $\text{molL}^{-1}$  of L-trypt followed by DPV method. The results did not find any interference effect for the detection L-trypt by using  $\text{Mg}^{2+}$ ,  $\text{K}^+$ ,  $\text{Ca}^{2+}$ ,  $\text{Cl}^-$ ,  $\text{SO}_4^{2-}$ ,  $\text{NO}_3^-$  and uric acid medium more than 200 fold (Fig. 6A). A negligible effect (less than 3%) was observed using the developed sensor for the detection of L-trypt in presence of interfering salt solution. In the

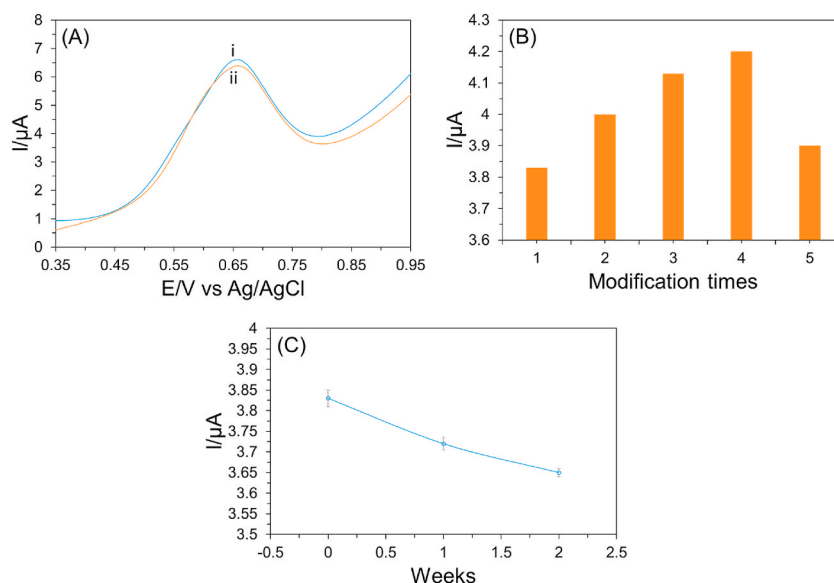


**Fig. 6.** A) DPV of GCE/CuONFs/PGA electrode i)  $1.0 \times 10^{-4} \text{ mol L}^{-1}$  L-trypt, ii)  $1.0 \times 10^{-4} \text{ mol L}^{-1}$  L-trypt in 200 fold interfering medium; B) Repetitive DPV current responses of GCE/CuONFs/PGA in 0.01 M PBS pH 7.0) consisting  $1.0 \times 10^{-4} \text{ mol L}^{-1}$  L-trypt and C) deviation of current response of GCE/CuONFs/PGA electrode in  $1.0 \times 10^{-4} \text{ mol L}^{-1}$  L-trypt in different weeks.

following step, a series of DPV measurements were evaluated with the concentration of  $1.0 \times 10^{-4} \text{ mol L}^{-1}$  to determine the reproducibility and the calculated standard deviation at  $n = 3$  were 0.3 and 0.2%, respectively (Fig. 6B). That means the reproducibility of the sensor was excellent. To evaluate the stability of the proposed sensor, the sensor was tested by storing at  $4^\circ\text{C}$  for two weeks and then tested  $1.0 \times 10^{-4} \text{ mol L}^{-1}$  of L-trypt solution. It can be seen that no significant change (less than 1.4%) was observed after two weeks which indicates the excellent stability of the proposed sensor (Fig. 6C).

### 3.7. Detection of L-trypt in milk and urine sample

Real sample detection is the most acceptable parameter to evaluate the performance of electrochemical sensor. In biological media the co-existing molecule can influence for the detection of target molecules. Hence, we have utilized our GCE/CuONFs/PGA modified electrode for the detection of L-trypt in real samples such as milk, and urine. To prepare the real sample, initially 1 mL of centrifuged milk sample was dispersed in 0.01 M PBS solution (pH 7.0) and thereafter  $1.0 \times 10^{-4} \text{ mol L}^{-1}$  and  $5.0 \times 10^{-5} \text{ mol L}^{-1}$  of L-trypt spiked in it and then applied for electrochemical sensing [77–79]. Similarly, a urine sample was also used as a real medium for the detection of  $1.0 \times 10^{-4} \text{ mol L}^{-1}$  and  $5.0 \times 10^{-5} \text{ mol L}^{-1}$  of L-trypt at the above condition. The obtained data are represented in the following Table 2. Based on data analysis, the recovery (%) and relative standard deviation were satisfactory for the real sample medium which was main aspect of this research study.

## 4. Conclusions

In summary, we have successfully developed a simple GCE/CuONFs/PGA electrochemical sensor to overcome the lack of sensitivity, selectivity, and time consuming analytical procedure. In this study, we developed a new route to synthesize CuONFs on the surface of GCE. The modified GCE/CuONFs/PGA electrode was applied to detect the L-trypt by using the differential pulse voltammetric technique to obtain individual peak responses. During detection, we are able to detect the lowest limit of  $5.0 \times 10^{-8} \text{ mol L}^{-1}$  of L-trypt. Furthermore, the modified GCE/CuONFs/PGA electrode exhibited higher electrocatalytic activity, good efficiency, better stability, and reproducibility towards L-trypt detection. Therefore, this study suggests that the developed sensor has a potential platform for the diagnosis of biological samples. The sample may be practiced for L-trypt analysis in clinical diagnosis even though having some limitations. Thus further extensive studies will be required for point-of-care applications with proper instrumentation of efficient electrochemical devices.

### Author contribution statement

M. Z. H. Khan conceived and planned this research work; M. A. Khaleque designed, performed the experimental work, and wrote the manuscript; M. S. Bacchu analyzed and interpreted the data; and M. R. Ali analyzed and interpreted the data. M. S. Hossain performed the experimental work; M. R. A. Mamun reviewed and edit the manuscript; M. I. Hossain reviewed and edit the manuscript.

**Table 2**  
Comparison of L-trypt in milk and urine as real samples.

Samples name	Spiked L-trypt (mol L <sup>-1</sup> )	Obtained current (μA)	Found L-trypt (mol L <sup>-1</sup> )	Recovery (%)	RSD (%)
Milk	1.0 × 10 <sup>-4</sup>	3.98	9.7 × 10 <sup>-4</sup>	97	1.83
	5.0 × 10 <sup>-5</sup>	2.1	4.9 × 10 <sup>-5</sup>	98	1.99
Urine	1.0 × 10 <sup>-4</sup>	4.05	9.8 × 10 <sup>-4</sup>	98	2.01
	5.0 × 10 <sup>-5</sup>	2.07	4.91 × 10 <sup>-5</sup>	98.2	2.00

### Funding statement

This research did not receive any specific funding facilities.

### Data availability statement

Data will be made available on request.

### Declaration of competing interest

The authors declare that there is no conflict of interest.

### References

- [1] O.J. D'Souza, R.J. Mascarenhas, T. Thomas, I.N.N. Namboothiri, M. Rajamathi, P. Martis, J. Dalhalle, Electrochemical determination of L-Tryptophan based on a multiwall carbon nanotube/Mg-Al layered double hydroxide modified carbon paste electrode as a sensor, *J. Electroanal. Chem.* 704 (2013) 220–226, <https://doi.org/10.1016/j.jelechem.2013.07.009>.
- [2] S. Shahrokhian, M. Bayat, Pyrolytic graphite electrode modified with a thin film of a graphite/diamond nano-mixture for highly sensitive voltammetric determination of tryptophan and 5-hydroxytryptophan, *Microchim. Acta* 174 (2011) 361–366, <https://doi.org/10.1007/s00604-011-0631-2>.
- [3] A. Agazzi, F. De Ponti, R. De Giorgio, S.M. Candura, L. Anselmi, E. Cervio, Modulation of intestinal motility by serotonergic (5-HT) receptors.pdf 35 (2003) 590–595.
- [4] W. Heine, M. Radke, K.D. Wutzke, The significance of tryptophan in human nutrition, *Amino Acids* 9 (1995) 91–205, <https://doi.org/10.1007/BF00805951>.
- [5] S. Hao, Y. Avraham, O. Bonne, E.M. Berry, Separation-induced body weight loss, impairment in alternation behavior, and autonomic tone: effects of tyrosine, *Pharmacol. Biochem. Behav.* 68 (2001) 273–281, [https://doi.org/10.1016/S0091-3057\(00\)00448-2](https://doi.org/10.1016/S0091-3057(00)00448-2).
- [6] P. Nagaraja, H.S. Yathirajan, R.A. Vasantha, Highly sensitive reaction of tryptophan with p-phenylenediamine ANALYTICAL BIOCHEMISTRY, *Anal. Biochem.* 312 (2003) 157–161. [www.elsevier.com/locate/yabio](http://www.elsevier.com/locate/yabio).
- [7] D.M. Reynolds, Rapid and direct determination of tryptophan in water using synchronous fluorescence spectroscopy, *Water Res.* 37 (2003) 3055–3060, [https://doi.org/10.1016/S0043-1354\(03\)00153-2](https://doi.org/10.1016/S0043-1354(03)00153-2).
- [8] L. Zhang, Y. Li, H. Zhou, L. Li, Y. Wang, Y. Zhang, Determination of eight amino acids in mice embryonic stem cells by pre-column derivatization HPLC with fluorescence detection, *J. Pharmaceut. Biomed. Anal.* 66 (2012) 356–358, <https://doi.org/10.1016/j.jpba.2012.03.014>.
- [9] M.F. Dario, T.B. Freire, C.A.S. de Oliveira Pinto, M.S.A. Prado, A.R. Baby, M.V.R. Velasco, Tryptophan and kynurenine determination in human hair by liquid chromatography, *J. Chromatogr., B: Anal. Technol. Biomed. Life Sci.* 1065–1066 (2017) 59–62, <https://doi.org/10.1016/j.jchromb.2017.09.020>.
- [10] L. Jiao, S. Bing, X. Zhang, Y. Wang, H. Li, Determination of enantiomeric composition of tryptophan by using fluorescence spectroscopy combined with backward interval partial least squares, *Anal. Methods* 7 (2015) 4535–4540, <https://doi.org/10.1039/c5ay00190k>.
- [11] Z. Lin, X. Chen, Z. Cai, P. Li, X. Chen, X. Wang, Chemiluminescence of tryptophan and histidine in Ru(bpy)<sub>3</sub><sup>2+</sup>-KMnO<sub>4</sub> aqueous solution, *Talanta* 75 (2008) 544–550, <https://doi.org/10.1016/j.talanta.2007.11.049>.
- [12] F.J.V. Gomez, A. Martín, M.F. Silva, A. Escarpa, Microchip electrophoresis-single wall carbon nanotube press-transferred electrodes for fast and reliable electrochemical sensing of melatonin and its precursors, *Electrophoresis* 36 (2015) 1880–1885, <https://doi.org/10.1002/elps.201400580>.
- [13] M.R. Ali, M.S. Bacchu, M.R. Al-Mamun, M.S. Ahommed, M.A. Saad Aly, M.Z.H. Khan, N-Hydroxysuccinimide crosslinked graphene oxide-gold nanoflower modified SPE electrode for sensitive detection of chloramphenicol antibiotic, *RSC Adv.* 11 (2021) 15565–15572, <https://doi.org/10.1039/d1ra02450g>.
- [14] Z.A. Khan, P.J.S. Hong, C.H. Lee, Y. Hong, Recent advances in electrochemical and optical sensors for detecting tryptophan and melatonin, *Int. J. Nanomed.* 16 (2021) 6861–6888, <https://doi.org/10.2147/IJN.S325099>.
- [15] Q. He, Y. Tian, Y. Wu, J. Liu, G. Li, P. Deng, D. Chen, Electrochemical sensor for rapid and sensitive detection of tryptophan by a Cu<sub>2</sub>O nanoparticles-coated reduced graphene oxide nanocomposite, *Biomolecules* 9 (2019), <https://doi.org/10.3390/biom9050176>.
- [16] S. Zhu, J. Zhang, X. en Zhao, H. Wang, G. Xu, J. You, Electrochemical behavior and voltammetric determination of L-tryptophan and L-tyrosine using a glassy carbon electrode modified with single-walled carbon nanohorns, *Microchim. Acta* 181 (2014) 445–451, <https://doi.org/10.1007/s00604-013-1138-9>.
- [17] K. Khoshnevisan, F. Torabi, H. Baharifar, S.M. Sajjadi-Jazi, M.S. Afjeh, F. Faridbod, B. Larjani, M.R. Khorramizadeh, Determination of the biomarker L-tryptophan level in diabetic and normal human serum based on an electrochemical sensing method using reduced graphene oxide/gold nanoparticles/18-crown-6, *Anal. Bioanal. Chem.* 412 (2020) 3615–3627, <https://doi.org/10.1007/s00216-020-02598-5>.
- [18] A.V. Porifreva, V.V. Gorbachuk, V.G. Evtugyn, I.I. Stoikov, G.A. Evtugyn, Glassy carbon electrode modified with silver nanodendrites implemented in polylactide-thiacalix[4]arene copolymer for the electrochemical determination of tryptophan, *Electroanalysis* 30 (2018) 641–649, <https://doi.org/10.1002/elan.201700638>.
- [19] S. Boonchiangma, S. Srijaranai, T. Tuntulani, W. Ngeontae, A highly selective electrochemical sensor for L-tryptophan based on a screen-printed carbon electrode modified with poly-p-phenylenediamine and CdS quantum dots, *J. Appl. Polym. Sci.* 131 (2014) 1–8, <https://doi.org/10.1002/app.40356>.
- [20] S. Nations, M. Long, M. Wages, J.D. Maul, C.W. Theodorakis, G.P. Cobb, Subchronic and chronic developmental effects of copper oxide (CuO) nanoparticles on *Xenopus laevis*, *Chemosphere* 135 (2015) 166–174, <https://doi.org/10.1016/j.chemosphere.2015.03.078>.
- [21] F. Perreault, S.P. Melegari, C.H. da Costa, A.L. de Oliveira Franco Rossetto, R. Popovic, W.G. Matias, Genotoxic effects of copper oxide nanoparticles in Neuro 2A cell cultures, *Sci. Total Environ.* 441 (2012) 117–124, <https://doi.org/10.1016/j.scitotenv.2012.09.065>.
- [22] S.M.S.I. Dulal, M.-S. Won, Y.-B. Shim, Characterisation of platinum nanoparticles electrodeposited on carbon felt, *J. Sci. Res.* 2 (2010) 303–312, <https://doi.org/10.3329/jsr.v2i2.3633>.
- [23] S. Reddy, B.E. Kumara Swamy, S. Aruna, M. Kumar, R. Shashanka, H. Jayadevappa, Preparation of NiO/ZnO Hybrid Nanoparticles for Electrochemical Sensing of Dopamine and Uric Acid, 2012. [www.simplex-academic-publishers.com](http://www.simplex-academic-publishers.com).
- [24] R. Shashanka, D. Chaira, B.E. Kumara Swamy, Electrochemical investigation of duplex stainless steel at carbon paste electrode and its application to the detection of dopamine, ascorbic and uric acid, *Int. J. Sci. Eng. Res.* (2015) 6. <http://www.ijser.org>.

- [25] R. Shashanka, D. Chaira, B. Kumara Swamy, Fabrication of yttria dispersed duplex stainless steel electrode to determine dopamine, ascorbic and uric acid electrochemically by using cyclic voltammetry, *Int. J. Sci. Eng. Res.* (2016) 7. <http://www.ijser.org>.
- [26] G. M, R.J. Mascarenhas, B.M. Basavaraja, Sensitive-selective determination of Propyl Paraben preservative based on synergistic effects of polyaniline-zinc-oxide nano-composite incorporated into graphite paste electrode, *Colloids Surf. B Biointerfaces* 184 (2019), 110529, <https://doi.org/10.1016/j.colsurfb.2019.110529>.
- [27] S.D. Bukkitgar, N.P. Shetti, R.M. Kulkarni, K.R. Reddy, S.S. Shukla, V.S. Saji, T.M. Aminabhavi, Electro-catalytic behavior of Mg-doped ZnO nano-flakes for oxidation of anti-inflammatory drug, *J. Electrochem. Soc.* 166 (2019), <https://doi.org/10.1149/2.0131909jes>. B3072–B3078.
- [28] V. Erady, R.J. Mascarenhas, A.K. Satpati, A.K. Bhakta, Z. Mekhalif, J. Delhalle, A. Dhason, Carbon paste modified with Bi decorated multi-walled carbon nanotubes and CTAB as a sensitive voltammetric sensor for the detection of Caffeic acid, *Microchem. J.* 146 (2019) 73–82, <https://doi.org/10.1016/j.microc.2018.12.023>.
- [29] S.D. Bukkitgar, N.P. Shetti, Electrochemical behavior of anticancer drug 5-fluorouracil at carbon paste electrode and its analytical application, *J. Anal. Sci. Technol.* 7 (2016) 1–9, <https://doi.org/10.1186/s40543-015-0080-3>.
- [30] G. Manasa, A.K. Bhakta, Z. Mekhalif, R.J. Mascarenhas, Voltammetric study and rapid quantification of resorcinol in hair dye and biological samples using ultrasensitive maghemite/MWCNT modified carbon paste electrode, *Electroanalysis* 31 (2019) 1363–1372, <https://doi.org/10.1002/elan.201900143>.
- [31] R. Shashanka, B.E. Kumara Swamy, Simultaneous electro-generation and electro-deposition of copper oxide nanoparticles on glassy carbon electrode and its sensor application, *SN Appl. Sci.* 2 (2020), <https://doi.org/10.1007/s42452-020-2785-1>.
- [32] N.P. Shetti, D.S. Nayak, S.J. Malode, K.R. Reddy, S.S. Shukla, T.M. Aminabhavi, Electrochemical behavior of flufenamic acid at amberlite XAD-4 resin and silver-doped titanium dioxide/amberlite XAD-4 resin modified carbon electrodes, *Colloids Surf. B Biointerfaces* 177 (2019) 407–415, <https://doi.org/10.1016/j.colsurfb.2019.02.022>.
- [33] P. Kalimuthu, S.A. John, Selective determination of 3,4-dihydroxyphenylacetic acid in the presence of ascorbic and uric acids using polymer film modified electrode, *J. Chem. Sci.* 123 (2011) 349–355, <https://doi.org/10.1007/s12039-011-0086-3>.
- [34] Z. Yu, X. Li, X. Wang, X. Ma, X. Li, K. Cao, Voltammetric determination of dopamine and norepinephrine on a glassy carbon electrode modified with poly (L-aspartic acid), *J. Chem. Sci.* 124 (2012) 537–544, <https://doi.org/10.1007/s12039-011-0179-z>.
- [35] A. Azadbakht, A. Abbasi, Acriflavine immobilized onto polyethyleneimine-wrapped carbon nanotubes/gold nanoparticles as an electrochemical sensing platform, *J. Chem. Sci.* 128 (2016) 257–268, <https://doi.org/10.1007/s12039-015-1029-1>.
- [36] C.L.P.S. Zanta, C.A. Martínez-Huitle, Electrochemical behaviour of platinum at polymer-modified glassy carbon electrodes, *J. Chem. Sci.* 119 (2007) 283–288, <https://doi.org/10.1007/s12039-007-0037-1>.
- [37] A. Pourjavadi, A.M. Harzandi, H. Hosseinzadeh, Modified carrageenan 3. Synthesis of a novel polysaccharide-based superabsorbent hydrogel via graft copolymerization of acrylic acid onto kappa-carrageenan in air, *Eur. Polym. J.* 40 (2004) 1363–1370, <https://doi.org/10.1016/j.eurpolymj.2004.02.016>.
- [38] H. Barrientos, I. Moggio, E. Arias-Marin, A. Ledezma, J. Romero, Layer-by-layer films of enzymatically synthesized poly(aniline)/bacterial poly( $\gamma$ -glutamic acid) for the construction of nanocapacitors, *Eur. Polym. J.* 43 (2007) 1672–1680, <https://doi.org/10.1016/j.eurpolymj.2007.02.038>.
- [39] S. Wu, F. Zeng, H. Zhu, S. Luo, B. Ren, Z. Tong, Mesomorphous structure and macroscopic patterns formed by polymer and surfactant from organic solutions, *Macromolecules* 38 (2005) 9266–9274, <https://doi.org/10.1021/ma051042g>.
- [40] M. Yoshikawa, K. Murakoshi, T. Kogita, K. Hanaoka, M.D. Guiver, G.P. Robertson, Chiral separation membranes from modified polysulfone having myrtenal-derived terpenoid side groups, *Eur. Polym. J.* 42 (2006) 2532–2539, <https://doi.org/10.1016/j.eurpolymj.2006.04.014>.
- [41] J. Xu, F. Zeng, S. Wu, X. Liu, C. Hou, Z. Tong, Gold nanoparticles bound on microgel particles and their application as an enzyme support, *Nanotechnology* 18 (2007), <https://doi.org/10.1088/0957-4484/18/26/265704>.
- [42] J.L. Audic, B. Chaufer, Influence of plasticizers and crosslinking on the properties of biodegradable films made from sodium caseinate, *Eur. Polym. J.* 41 (2005) 1934, <https://doi.org/10.1016/j.eurpolymj.2005.02.023>. –1942.
- [43] I. Porcar, A. Codoñer, C.M. Gómez, C. Abad, A. Campos, Interactions of quinine with polyacrylic and poly-L-glutamic acids in aqueous solutions, *Eur. Polym. J.* 40 (2004) 819–828, <https://doi.org/10.1016/j.eurpolymj.2003.11.011>.
- [44] Y. Liu, X. Dong, P. Chen, Biological and chemical sensors based on graphene materials, *Chem. Soc. Rev.* 41 (2012) 2283–2307, <https://doi.org/10.1039/c1cs15270j>.
- [45] A.M. Yu, H.Y. Chen, Electrocatalytic oxidation and determination of ascorbic acid at poly(glutamic acid) chemically modified electrode, *Anal. Chim. Acta* 344 (1997) 181–185, [https://doi.org/10.1016/S0003-2670\(97\)00016-0](https://doi.org/10.1016/S0003-2670(97)00016-0).
- [46] Y. Zhang, L. Luo, Y. Ding, X. Liu, Z. Qian, A highly sensitive method for determination of paracetamol by adsorptive stripping voltammetry using a carbon paste electrode modified with nanogold and glutamic acid, *Microchim. Acta* 171 (2010) 133–138, <https://doi.org/10.1007/s00604-010-0422-1>.
- [47] G.H. Ho, T.I. Ho, K.H. Hsieh, Y.C. Su, P.Y. Lin, J. Yang, K.H. Yang, S.C. Yang,  $\gamma$ -polyglutamic acid produced by *Bacillus subtilis* (natto): structural characteristics, chemical properties and biological functionalities, *J. Chin. Chem. Soc.* 53 (2006) 1363–1384, <https://doi.org/10.1002/jccs.200600182>.
- [48] I.L. Shih, Y.T. Van, The production of poly( $\gamma$ -glutamic acid) from microorganisms and its various applications, *Bioresour. Technol.* 79 (2001) 207–225, [https://doi.org/10.1016/S0960-8524\(01\)00074-8](https://doi.org/10.1016/S0960-8524(01)00074-8).
- [49] M. Nagasawa, A. Holtzer, The helix-coil transition in solutions of polyglutamic acid, *J. Am. Chem. Soc.* 86 (1964) 538–543, <https://doi.org/10.1021/ja01058a002>.
- [50] S. Saif, A. Tahir, T. Asim, Y. Chen, Plant mediated green synthesis of CuO nanoparticles: comparison of toxicity of engineered and plant mediated CuO nanoparticles towards *Daphnia magna*, *Nanomaterials* 6 (2016) 1–15, <https://doi.org/10.3390/nano6110205>.
- [51] N.C. Horti, M.D. Kamatagi, N.R. Patil, M.S. Sannaikar, S.R. Inamdar, Synthesis and optical properties of copper oxide nanoparticles: effect of solvents, *J. Nanophotonics* 14 (2020) 1–9, <https://doi.org/10.1117/1.jnp.14.046010>.
- [52] F. Liu, L. Csetenyi, G.M. Gadd, Amino acid secretion influences the size and composition of copper carbonate nanoparticles synthesized by ureolytic fungi, *Appl. Microbiol. Biotechnol.* 103 (2019) 7217–7230, <https://doi.org/10.1007/s00253-019-09961-2>.
- [53] S.D. Giri, A. Sarkar, Electrochemical study of bulk and monolayer copper in alkaline solution, *J. Electrochem. Soc.* 163 (2016), <https://doi.org/10.1149/2.0071605jes>. H252–H259.
- [54] L. Wang, P. Huang, J. Bai, H. Wang, L. Zhang, Y. Zhao, Direct simultaneous electrochemical determination of hydroquinone and catechol at a poly(glutamic acid) modified glassy carbon electrode, *Int. J. Electrochem. Sci.* 2 (2007) 123–132.
- [55] M. Yesil, S. Donmez, F. Arslan, Development of an electrochemical DNA biosensor for detection of specific *Mycobacterium tuberculosis* sequence based on poly (L-glutamic acid) modified electrode, *J. Chem. Sci.* 128 (2016) 1823–1829, <https://doi.org/10.1007/s12039-016-1159-0>.
- [56] S. Chitravathi, B.E.K. Swamy, G.P. Mamatha, B.S. Sherigara, Simultaneous electrochemical determination of dopamine and ascorbic acid using poly (l-serine) modified carbon paste electrode, *J. Mol. Liq.* 160 (2011) 193–199, <https://doi.org/10.1016/j.molliq.2011.03.019>.
- [57] L. Huang, E.S. Lee, K.B. Kim, Electrodeposition of monodisperse copper nanoparticles on highly oriented pyrolytic graphite electrode with modulation potential method, *Colloids Surf. A Physicochem. Eng. Asp.* 262 (2005) 125–131, <https://doi.org/10.1016/j.colsurfa.2005.03.023>.
- [58] F.E. Heikal, O.S. Shehata, N.S. Tantawy, A.M. Fekry, Investigation on the corrosion and hydrogen evolution for AZ91D magnesium alloy in single and anion-containing oxalate solutions, *Int. J. Hydrogen Energy* 37 (2011) 84–94, <https://doi.org/10.1016/j.ijhydene.2011.08.051>.
- [59] A.M. Fekry, M. Shehata, S.M. Azab, A. Walcarius, Jo ur l P re of, *Sensor. Actuator. B Chem.* (2019), 127172, <https://doi.org/10.1016/j.snb.2019.127172>.
- [60] B. Applications, *Electrochemical Impedance Spectroscopy (EIS): Principles, Construction, and Biosensing Applications*, 2021.
- [61] W. Yi, Z. He, J. Fei, X. He, Sensitive electrochemical sensor based on poly(L-glutamic acid)/graphene oxide composite material for simultaneous detection of heavy metal ions, *RSC Adv.* 9 (2019) 17325–17334, <https://doi.org/10.1039/c9ra01891c>.
- [62] S.D. GunaVathana, P. Thivya, J. Wilson, A.C. Peter, Sensitive voltammetric sensor based on silver dendrites decorated polythiophene nanocomposite: selective determination of L-Tryptophan, *J. Mol. Struct.* 1205 (2020), 127649, <https://doi.org/10.1016/j.molstruc.2019.127649>.

- [63] G.P. Jin, X.Q. Lin, Erratum: the electrochemical behavior and amperometric determination of tyrosine and tryptophan at a glassy carbon electrode modified with butyrylcholine, *Electrochem. Commun.* 6 (2004) 454–460, <https://doi.org/10.1016/j.elecom.2004.05.014>. *Electrochemistry Communications*. 6 (2004) 742.
- [64] M. Xu, M. Ma, Y. Ma, Electrochemical determination of tryptophan based on silicon dioxide nanopartilces modified carbon paste electrode, *Russ. J. Electrochem.* 48 (2012) 489–494, <https://doi.org/10.1134/S1023193512050126>.
- [65] X. Tang, Y. Liu, H. Hou, T. You, Electrochemical determination of L-Tryptophan, L-Tyrosine and L-Cysteine using electrospun carbon nanofibers modified electrode, *Talanta* 80 (2010) 2182–2186, <https://doi.org/10.1016/j.talanta.2009.11.027>.
- [66] X. Liu, L. Luo, Y. Ding, D. Ye, Poly-glutamic acid modified carbon nanotube-doped carbon paste electrode for sensitive detection of L-tryptophan, *Bioelectrochemistry* 82 (2011) 38–45, <https://doi.org/10.1016/j.bioelechem.2011.05.001>.
- [67] D. Sun, H. Li, M. Li, C. Li, H. Dai, D. Sun, B. Yang, Electrodeposition synthesis of a NiO/CNT/PEDOT composite for simultaneous detection of dopamine, serotonin, and tryptophan, *Sensor. Actuator. B Chem.* 259 (2018) 433–442, <https://doi.org/10.1016/j.snb.2017.12.037>.
- [68] B. Kaur, B. Satpati, R. Srivastava, Synthesis of NiCo<sub>2</sub>O<sub>4</sub>/Nano-ZSM-5 nanocomposite material with enhanced electrochemical properties for the simultaneous determination of ascorbic acid, dopamine, uric acid and tryptophan, *New J. Chem.* 39 (2015) 1115–1124, <https://doi.org/10.1039/c4nj01360c>.
- [69] F.H. Narouei, H.K. Tammandani, Y. Ghalandarzehi, N. Sabbaghi, M. Noroozifar, An electrochemical sensor based on conductive polymers/graphite paste electrode for simultaneous determination of dopamine, uric acid and tryptophan in biological samples, *Int. J. Electrochem. Sci.* 12 (2017) 7739–7753, <https://doi.org/10.20964/2017.08.50>.
- [70] C.X. Xu, K.J. Huang, Y. Fan, Z.W. Wu, J. Li, T. Gan, Simultaneous electrochemical determination of dopamine and tryptophan using a TiO<sub>2</sub>-graphene/poly(4-aminobenzenesulfonic acid) composite film based platform, *Mater. Sci. Eng. C* 32 (2012) 969–974, <https://doi.org/10.1016/j.msec.2012.02.022>.
- [71] T. Thomas, R.J. Mascarenhas, O.J. D'Souza, P. Martis, J. Dalhalla, B.E. Kumara Swamy, Multi-walled carbon nanotube modified carbon paste electrode as a sensor for the amperometric detection of l-tryptophan in biological samples, *J. Colloid Interface Sci.* 402 (2013) 223–229, <https://doi.org/10.1016/j.jcis.2013.03.059>.
- [72] K.Q. Deng, J. hong Zhou, X.F. Li, Direct electrochemical reduction of graphene oxide and its application to determination of l-tryptophan and l-tyrosine, *Colloids Surf. B Biointerfaces* 101 (2013) 183–188, <https://doi.org/10.1016/j.colsurfb.2012.06.007>.
- [73] Y. Zhang, G.I.N. Waterhouse, Z. peng Xiang, J. Che, C. Chen, W. Sun, A highly sensitive electrochemical sensor containing nitrogen-doped ordered mesoporous carbon (NOMC) for voltammetric determination of L-tryptophan, *Food Chem.* 326 (2020), <https://doi.org/10.1016/j.foodchem.2020.126976>.
- [74] J. Han, J. Zhao, Z. Li, H. Zhang, Y. Yan, D. Cao, G. Wang, Nanoporous carbon derived from dandelion pappus as an enhanced electrode material with low cost for amperometric detection of tryptophan, *J. Electroanal. Chem.* 818 (2018) 149–156, <https://doi.org/10.1016/j.jelechem.2018.04.044>.
- [75] G.A. Tig, Development of electrochemical sensor for detection of ascorbic acid, dopamine, uric acid and L-tryptophan based on Ag nanoparticles and poly(L-arginine)-graphene oxide composite, *J. Electroanal. Chem.* 807 (2017) 19–28, <https://doi.org/10.1016/j.jelechem.2017.11.008>.
- [76] Y. Wang, D. Li, J. Kang, S. Guan, D. Wu, An electrochemical sensor based on MB/Ag-ZnO/graphene modified glassy carbon electrode for determination of L-tryptophan in biofluid samples, *Int. J. Electrochem. Sci.* 14 (2016) 5448–5461, <https://doi.org/10.20964/2019.06.29>.
- [77] J.V. Kumar, R. Karthik, S.M. Chen, S. Marikkani, A. Elangovan, V. Muthuraj, Green synthesis of a novel flower-like cerium vanadate microstructure for electrochemical detection of tryptophan in food and biological samples, *J. Colloid Interface Sci.* 496 (2017) 78–86, <https://doi.org/10.1016/j.jcis.2017.02.009>.
- [78] R. Sakthivel, B. Mutharani, S.-M. Chen, S. Kubendhiran, T.-W. Chen, F.M.A. Al-Hemaid, M.A. Ali, M.S. Elshikh, A simple and rapid electrochemical determination of L-tryptophan based on functionalized carbon black/poly-L-histidine nanocomposite, *J. Electrochem. Soc.* 165 (2018) B422–B430, <https://doi.org/10.1149/2.0381810jes>.
- [79] Y. Liu, L. Xu, Electrochemical sensor for tryptophan determination based on copper-cobalt hexacyanoferrate film modified graphite electrode, *Sensors* 7 (2007) 2446–2457, <https://doi.org/10.3390/s7102446>.